

Topical Review

Superconductivity in interacting interfaces of cuprate-based heterostructures

Daniele Di Castro  and Giuseppe Balestrino 

CNR-SPIN and Dipartimento di Ingegneria Civile e Ingegneria Informatica, Università di Roma Tor Vergata, via del Politecnico 1, 00133 Italy

E-mail: daniele.di.castro@uniroma2.it

Received 19 January 2017, revised 17 April 2018

Accepted for publication 3 May 2018

Published 6 June 2018



Abstract

Low dimensional superconducting systems have been the subject of numerous studies in the recent past, with the aim of achieving a higher and higher critical temperature (T_c). The recent improvement in film deposition techniques has allowed the realization of artificial heterostructures, with atomically flat surfaces and interfaces, where novel properties appear that are not present in the single constituent. For instance, quasi-2D superconductivity was found at the interface between different oxides. In this review we analyze, in particular, the quasi-2D superconductivity occurring at the interface between two non-superconducting oxides, mostly cuprates. Throughout a comparison of the superconducting properties of different oxide heterostructures and superlattices, we propose a phenomenological explanation of the behavior of the T_c as a function of the number of conducting CuO₂ planes. This is achieved by introducing two different interactions between the superconducting 2D sheets. This interpretation is finally extended also to standard high T_c cuprates, contributing to the solution of the long-standing question of the dependence of T_c on the number of CuO₂ planes in these systems.

Keywords: superconductivity, interface, high T_c superconductors, film deposition, low dimensionality

(Some figures may appear in colour only in the online journal)

1. Introduction

The increase of the critical temperature T_c in superconducting materials and the search for novel superconducting systems have been, in the past half-century, among the most aimed-at goals in condensed matter physics and materials science. Indeed, higher T_c and appropriately engineered materials could allow the development of a plethora of possible technological applications, from novel electronic devices to power transmission.

In this scenario, one long-standing idea is that, despite the increased role of fluctuations, enhanced T_c may be achieved in low dimensional electronic systems [1, 2]. For example, it could be realized at the surface of a material, at the interface between different materials, or at the boundary between different phases or crystallographic orientations within one material. In fact, apart from the very recent discovery of the occurrence of a

superconducting phase at 200 K in sulfur hydride systems under ultrahigh pressures (up to 150 GPa) [3, 4], the highest T_c materials found up until now can be grouped into two families: the cuprates, with T_c of up to 164 K [5] (in HgBa₂Ca₂Cu₃O₉ at 30 GPa), and Fe-pnictides and -chalcogenides (FPC) with T_c of up to 55 K [6]. One common feature of these families of superconductors, and, actually, of all superconductors with a T_c higher than about 30 K, is a layered structure, where the superconductivity occurs in quasi-two-dimensional (q2D) active subsystems. The discovery of high T_c in these ‘natural superlattices’ has refreshed interest in the realization of low dimensional superconducting systems. The concomitant strong improvement in film deposition techniques such as molecular beam epitaxy (MBE), pulsed laser deposition (PLD), multi-target sputtering and co-evaporation, has allowed the engineering of high-quality artificial heterostructures with atomically flat

surfaces and interfaces. The realization of 2D structures, envisaged long ago, has become possible.

The large body of experiments performed up until now, often supported by both old and more recent theoretical predictions, has led to the finding of two classes of phenomena occurring at the surface of a material or at the interface between two different materials: (i) a T_c enhancement, in systems where at least one (or the unique) constituent is a superconductor, and; (ii) the occurrence of superconductivity in systems where both (the unique) constituents (constituent) are (is) non-superconducting.

To the first class we can ascribe, for example, the pioneering works of Strongin and Kammerer [7], where they show a T_c of about 6 K in an Al/Al₂O₃ heterostructure, or the twinning-plane superconductivity (TPS), where superconductivity localized around the twin planes occurs at a T_c higher than the critical temperature of the bulk metal [8]. To this class belongs also the very surprising recent report of Ge and collaborators on high T_c superconductivity (T_c about 100 K) found in a one-unit cell FeSe film grown on a SrTiO₃ substrate [9]. This enhancement of the critical temperature, occurring when a superconducting film is coupled to another material, the latter being superconducting or not, revealed the fact that a phase, different from the bulk, is formed at the interface between the two systems. However, a full consensus on the mechanism at the base of the T_c enhancement occurring in ultrathin FeSe has not been reached yet. Some authors have attributed it to an enhancement of the electron–phonon interaction at the interface with the substrate [10]. More recently a different explanation was given of the enhancement in the transition temperature in ultrathin layers, based on the opening of an additional superconducting gap, while retaining a largely unchanged ‘bulk’ superconducting gap [11]. This latter mechanism is not strictly connected to the interface, as it would depend only on the thickness of the film.

The second class of phenomena comprises the occurrence of superconductivity at the interface between two non-superconducting systems. In particular, interface superconductivity has been shown in heterostructures formed by a non-superconducting metal and an insulator, as, for example, CaCuO₂/BaCuO_{2+d}, with $T_c \approx 80$ K, reported in the earlier works of Balestrino *et al* [12], or La_{1.55}Sr_{0.45}CuO₄/La₂CuO₄, with $T_c \approx 30$ K, as shown in the more recent report by Gozar *et al* [13]. Very strikingly, even the interface between two insulator materials could give rise to a superconducting phase, as shown in a LaAlO₃/SrTiO₃ heterostructure [14] ($T_c \approx 0.2$ K), in a LaTiO₃/SrTiO₃ heterostructure [15] ($T_c \approx 0.3$ K), and, more recently, in CaCuO₂/SrTiO₃ heterostructures [16] ($T_c = 38$ K).

The exact mechanism at the base of the occurrence of interface superconductivity in all these heterostructures, as well as of the high T_c superconductivity in single phase systems (cuprates, pnictides, etc), is still highly debated. Indeed, interaction at the interface comprises a variety of effects such as epitaxial strain, interface defects, elemental interdiffusion, interface charge layers, electrical charge transfer between layers, and others. Each one of these effects can affect the superconducting properties of the interface.

The possibility now to explore these phenomena by artificially creating ad hoc interfaces will likely lead to new

and important insights into this exciting field of physics, and, more optimistically, to the engineering of superconductors with record high T_c and better applicative properties.

In this review we will focus on the second class of phenomena, and, in particular, on interface superconductivity between two non-superconducting oxides, mostly cuprates, where a large quantity of experimental evidence has been collected and a satisfactory phenomenological understanding of the phenomenon reached. We will compare the superconducting properties of the individual interfaces for different oxide systems. Successively, we will introduce interaction among different superconducting interfaces in heterostructures and superlattices (SLs) and will check the effect of such an interaction on the 2D character of superconductivity. For further details on the general problem of interface superconductivity we direct readers to two recently published review papers [17, 18]. As for the ultrathin FeSe film and LAO/STO heterostructure, excellent recent reviews are given in [18 and 19], respectively. At the end of this review, we will try to find common features in the different classes of materials considered and will mention some ideas and proposals for future developments.

2. CaCuO₂/SrTiO₃

It has been recently shown that a variety of extraordinary phenomena, not present in the single constituent, can occur at the interface between two insulating oxides [13–16, 20–24]. For instance, a conducting 2D electron gas sets in at the LaAlO₃/SrTiO₃ interface and, in addition, superconductivity appears at $\sim 10^{-1}$ K [14], the transition temperature of which can be modulated via electric field control of the carrier density [24]. From this finding, the idea arose that conducting interfaces could be used as a charge reservoir to dope a cuprate with an ‘infinite layers’ (IL) structure, with the aim of achieving much higher T_c values.

Indeed, the layered cuprate high T_c superconductors (HTS) can be considered as being constituted of a sequence of two different blocks: a block with an IL structure (i.e., a sequence of CuO₂ planes and Ca planes stacked along the *c*-axis) and a charge reservoir (CR) block that can be doped by excess oxygen ions or chemical substitution, thus providing charges to the IL block (see figure 1).

Following this scheme, we can mimic the behavior of standard HTS compounds by realizing a CR at the interface between a cuprate and another oxide.

We have explored such a possibility by realizing, by means of PLD, artificial superlattices [(CaCuO₂)_{*n*}/(SrTiO₃)_{*m*}]_{*N*}, made by *N* repetitions of *n* unit cells of CaCuO₂ (CCO) and *m* unit cells of SrTiO₃ (STO) [26, 27] (see figure 2).

CCO is an antiferromagnetic insulator [28] with an IL structure, where the CuO₂ planes are separated by bare Ca atoms, as in the IL blocks of HTS, and can be considered a parent compound of the HTS with the simplest lattice structure. The tetragonal phase of CCO, with $a = b = 3.86$ Å and $c = 3.20$ Å, can be stabilized in the form of a thin film by a good lattice match with perovskite substrates, in particular with NdGaO₃ [29], which has a pseudocubic lattice parameter

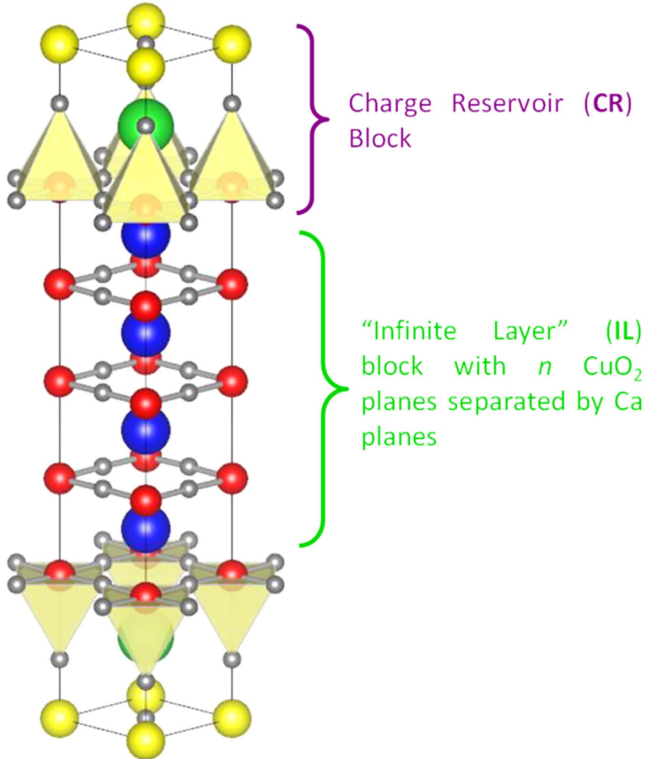


Figure 1. Schematic structure of Hg1245. The two different structural blocks, IL and CR, are highlighted. Reproduced with permission from [25].

3.87 Å. STO is an insulating perovskite. Thus, we actually substituted the LAO layer with CCO to form CCO/STO superlattices, instead of a LAO/STO heterostructure. In our SLs, we face the insulating IL CCO, which, containing the CuO_2 planes, can turn in a superconductor if doped with charge carriers, to the insulating perovskite STO. From this point of view, the CCO/STO interfaces are very similar to the IL/CR native interfaces occurring in HTS.

The CCO/STO superlattices were deposited on $5 \times 5 \text{ mm}^2$ NdGaO_3 (110) (NGO) oriented monocrystalline substrates by PLD (KrF excimer laser = 248 nm). A multi-target system was used, with CaCuO_2 and SrTiO_3 nominal composition targets. The superconducting SLs were grown in an oxygen and 12% ozone mixed atmosphere at a pressure of about 1 mbar (see [16, 26] and [27] for further details of the sample growth).

The quality of the crystallographic structure is checked by x-ray diffraction (XRD) and high-resolution transmission electron microscopy (HRTEM) measurements. Figure 2 reports, as an example, the XRD pattern and the HRTEM image of the superlattice $[(\text{CCO})_{3/4}/(\text{STO})_2]_{20}$ (where the subscript 3/4 indicates that there are some blocks of CCO with three unit cells and others with four unit cells, as shown in the inset of figure 2(c)). A heteroepitaxial superlattice and sharp interfaces are clearly evinced.

If grown in strongly oxidizing conditions (oxygen/12% ozone at $p \approx 1 \text{ mbar}$), the CCO/STO SLs are superconducting, with a maximum T_c (zero resistance temperature) of about 50 K [26, 27]. If individual CCO and STO films are

grown in the above strongly oxidizing conditions, these compounds retain their native insulating character. (See the resistance of CCO as a function of temperature in the inset of figure 3.)

This reveals that the occurrence of superconductivity is a new phenomenon arising at the interfaces between the two insulating systems.

Since superconductivity appears only if the film is grown in strongly oxidizing conditions, we explored the dependence of the sample resistivity on the growth conditions (figure 3(a)). The conductivity increases, going from pure oxygen at 0.2 mbar (green line) to pure oxygen at $\sim 1 \text{ mbar}$ (blue line), and to the oxygen/12% ozone mixture at $\sim 1 \text{ mbar}$ (red line). The last is superconducting with $T_c = 38 \text{ K}$. The T_c also varies with fine tuning of the growth conditions, with a maximum T_c of about 50 K (figure 3(b)) [27]. Thus, the occurrence of superconductivity should be related to the introduction of excess oxygen ions in the structure, which in turn induces charge doping in the CCO.

X-ray absorption spectroscopy (XAS) measurements at the Cu edge [31, 32] helped in understanding the doping mechanism. Indeed, measurements performed on superconducting and non-superconducting (grown at lower oxygen pressure) SLs (see figure 4) showed that the doping is realized by holes in the cuprate block (spectral weight D in figure 4) [26]. Given that: (i) superconductivity appears only if the SL is grown in strongly oxidizing conditions; (ii) the CCO alone cannot be a superconductor (see inset of figure 3), and therefore the presence of interfaces is crucial for the occurrence of superconductivity, at this stage we can formulate the hypothesis that the holes derive from the incorporation of extra oxygen ions at the interface between CCO and STO during the growth. This hypothesis will be demonstrated experimentally by the study of the bilayer CCO/STO discussed below.

On the other hand, the STO seems not to be involved in conductivity, since the Ti bands are not affected by the presence of extra oxygen ions, as seen in the $\text{Ti } L_{2,3}$ edges XAS spectra (inset of figure 4(b)). Thus, this case is actually different from the LAO/STO interface, where the Ti bands were involved in conductivity and the T_c was around 0.2 K [14].

The T_c of the SLs varies not only with the oxidizing conditions, but also with the number of CCO unit cells of the CCO block. In figure 5, recently measured values of T_c on a series of SLs, having the same number of STO unit cells $m = 2$ and different number (n) of CCO unit cells, are reported as a function of n .

A maximum of T_c is obtained for $3 < n < 4$, whereas for $n > 5$ a nearly constant value is observed. This behavior of T_c is typical of CCO/STO SLs [26], and, remarkably, it recalls the behavior shown by HTS cuprates [33], thus reinforcing the idea that the doping mechanism at the CCO/STO interface is similar to the one occurring at the IL/CR interfaces in HTS. This circumstance opens important perspectives for the comprehension of the phenomenological behavior of high T_c superconductivity in HTS through the study of CCO/STO heterostructures, as we will show in the following.

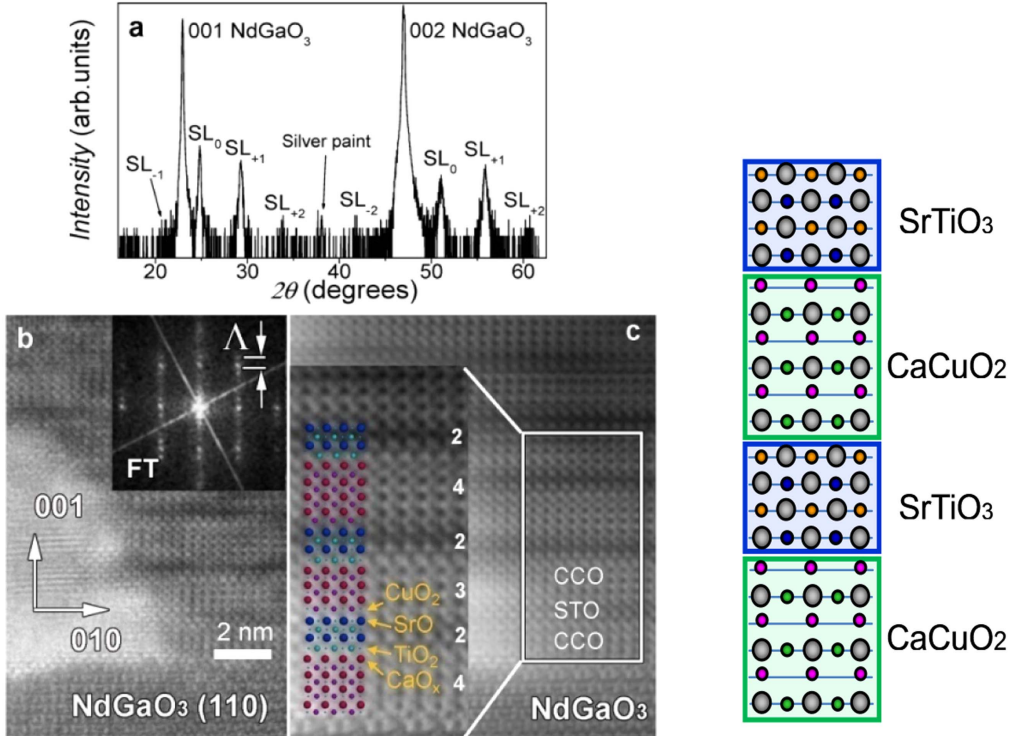


Figure 2. (a) XRD pattern from $(\text{CCO})_{3/4}/(\text{STO})_2$ SLs. SL_0 indicates the average structure peak and the $\text{SL}_{\pm l}$ mark the satellite peaks around it. The substrate peaks are also indicated with the pseudocubic notation for NGO. (b) HRTEM image of an identical SL taken along the [110] orientation (orthorhombic notation) of the NdGaO_3 substrate. Inset: Fourier transform pattern where superlattice spots are clearly visible. (c) Filtered HRTEM image. Inset: enlargement of the area marked by the white rectangle. An atomic model of STO-CCO sequences is superimposed (dark blue: Sr; light blue: Ti; small light blue: O; red: Ca; purple: Cu). Reprinted figure with permission [26], Copyright 2012 by the American Physical Society.

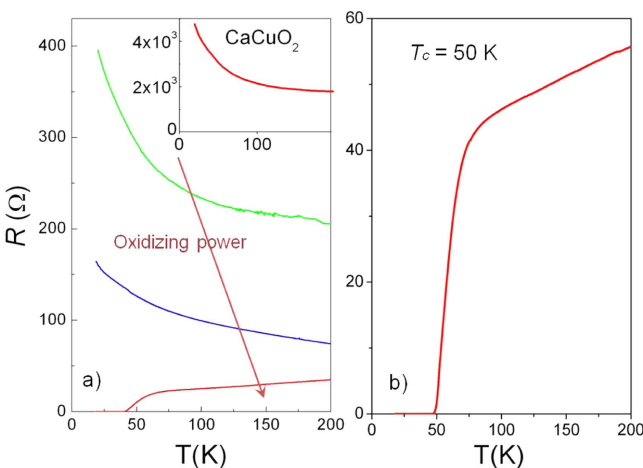


Figure 3. Temperature dependence of the resistance of the CCO film (inset of (a)), and CCO/STO SLs (a) grown at different oxidizing conditions: O₂ at 1×10^{-1} mbar (green line), O₂ at 8×10^{-1} mbar (blue line), O₂ + O₃ (12%) at 8×10^{-1} mbar (red line). (b) The best CCO/STO superlattice with the maximum T_c obtained, of 50 K. Adapted from [30] 2015 © Springer International Publishing Switzerland 2015. With permission of Springer. ‘Figure 3: Temperature dependence of the resistance for the CCO film (inset panel a), and CCO/STO SLs grown at different oxidizing conditions (panel a). b) the best CCO/STO superlattice with the maximum T_c obtained, 50 K’.

Returning to the XAS spectra reported in figure 4, we can observe, apart from the peak D , present in both the polarizations at the high energy side of the Cu L₃ absorption edge (peak U) and ascribed to the hole-doped Cu sites [26], an increased spectral weight (indicated by A in the figure) on the low energy side of U in the E//c spectrum for both the superconducting and non-superconducting $n = 3$ CCO/STO SLs. This feature was ascribed in [27] to the presence of apical oxygen ions at undoped Cu sites. Consequently, we can conclude that there are two different apical oxygens: excess oxygens, which provide holes doping, and stoichiometric oxygens, which do not provide doping. To better understand this point, we analyze the structure of the interfaces in CCO/STO SLs. Two kinds of interfaces are present: CuO₂-Ca-TiO₂ at the top interface of CCO with STO and TiO₂-SrO-CuO₂ at the bottom interface, as schematically shown in figures 6(a) and (b), respectively.

If the whole CCO block in CCO/STO retains an ideal IL structure, then the Cu ions can have apical oxygens only at the interface TiO₂-SrO-CuO₂, provided by the oxygen ions in the SrO planes. At the other interface, CuO₂-Ca-TiO₂, the Cu ions do not have apical oxygens, since in the IL structure no oxygen ions are present in the Ca planes. If the superlattice is grown in strongly oxidizing conditions, x extra oxygen ions

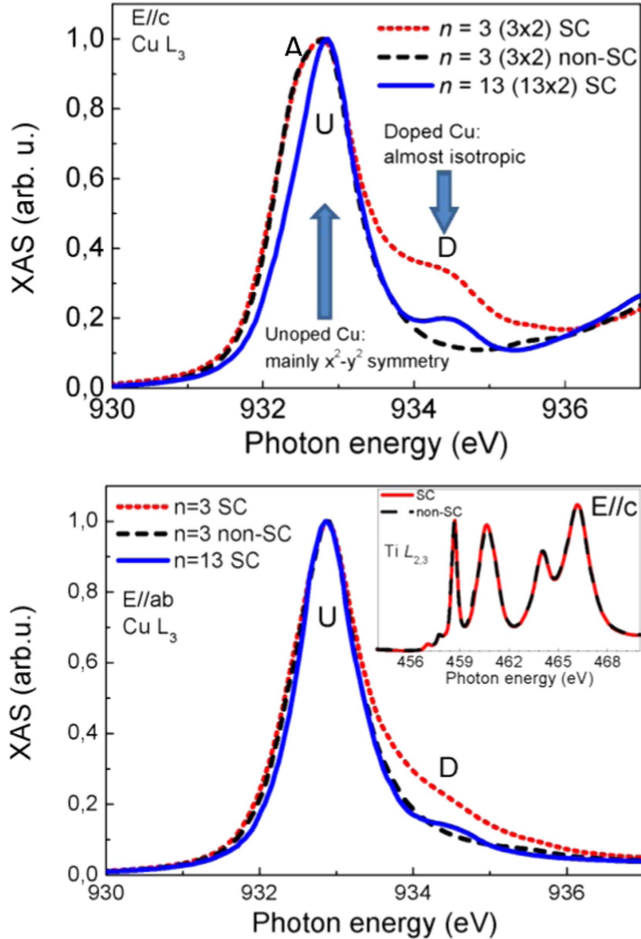


Figure 4. XAS spectra with $E//c$ (upper panel) and $E//ab$ (lower panel) of two superconducting superlattices, $\text{CCO}_3/\text{STO}_2$ and $\text{CCO}_{13}/\text{STO}_2$, and one non-superconducting superlattice $\text{CCO}_3/\text{STO}_2$. Inset: $Ti\text{ }L_{2,3}$ edges XAS spectra with $E//c$ for superconducting and non-superconducting SLs. Reprinted figure with permission from [26], Copyright 2012 by the American Physical Society. Reproduced from [27]. © IOP Publishing Ltd. All rights reserved.

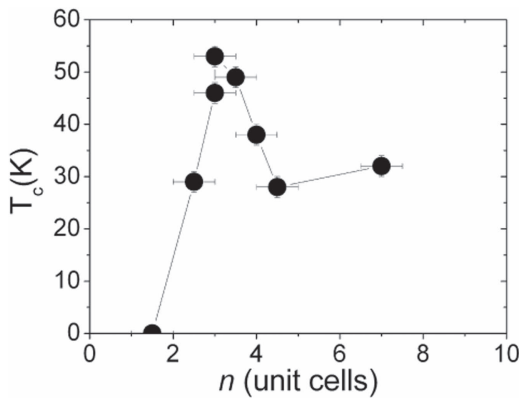


Figure 5. Dependence of T_c on the number n of CCO unit cells within the supercell, which corresponds to the number of CuO_2 planes, for a series of $(\text{CCO})_n/(\text{STO})_2$ SLs.

enter the interface Ca plane, forming the $\text{CuO}_2\text{-CaO}_x\text{-TiO}_2$ interface and doping with holes the neighbor CuO_2 planes. On the other hand, the apical oxygen ions in the interface SrO plane are stoichiometric, and thus do not dope. This

description is supported by the XAS spectra in figure 4 and, in turn, it helps in precisely assigning the spectral weights A and D . The spectral weight A , ascribed to the undoped Cu sites at the interface with the SrO plane of STO with stoichiometric apical O ions; the spectral weight D , ascribed to doped Cu sites [26], is due to the doped Cu sites with excess apical oxygens at the other interface. Indeed, the former is below the experimental sensitivity in the spectra of the superconducting SL with $n = 13$, where the relative weight of the interfaces is lower, and the latter is strongly suppressed in the $n = 13$ SL and is absent in the $n = 3$ non-superconducting SL.

In this framework, only one of the two interfaces in CCO/STO SLs is ‘active’. This conclusion was confirmed by the study of a single interface; that is, a bilayer CCO/STO .

Indeed, in this case, by growing the bilayer on Nd-terminated NdGaO_3 substrates, it is possible to select one of the two interfaces by choosing CCO or STO as the first block. The $\text{CuO}_2\text{-Ca-TiO}_2$ interface is realized if the CCO is deposited first (NGO/CCO/STO heterostructure), whereas the $\text{TiO}_2\text{-SrO-CuO}_2$ is realized in the other case (NGO/STO/CCO heterostructure). We found that only the former structure is superconducting, as shown by the temperature dependence of the resistance reported in figure 7 for NGO/(CCO)₄₀/(STO)₃₀, NGO/(STO)₁₀/(CCO)₄₀ bilayers.

This property was also checked by growing the trilayer NGO/(STO)₁₀/(CCO)₄₀/(STO)₃₀. In this case, since the CCO/STO interface is reproduced, the system is again superconducting (figure 7(a)).

The Sr/Ca interdiffusion at the CCO/STO interface as the origin of the superconducting behavior of Sr-doped CCO has been excluded by the fact that the bilayer NGO/(CCO)₄₀/(CTO)₃₀, where CTO is CaTiO_3 and no Sr atoms are present, is also superconducting, with a T_c similar to the CCO/STO bilayer (see figure 7(a)). Also, the possibility that the exposure of the top CCO to the air was responsible for the absence of a superconducting interface was tested by growing the bilayer NGO/(STO)₁₀/(CCO)₄₀/(STO)_{am} with a cap of an amorphous STO layer (STO)_{am}. As shown in figure 7(a), this system has a behavior similar to the NGO/STO/CCO with no cap, thus confirming that it is really a question of growth sequence.

In the NGO/CCO/STO bilayer ($\text{CuO}_2\text{-Ca-TiO}_2$ interface), extra oxygen ions can enter the Ca plane at the interface with the TiO_2 plane, as shown by the black dots in figure 7(b). The x extra apical oxygen ions in the CaO_x planes inject holes in the CuO_2 planes below, making the system superconducting, as already envisaged by the study of CCO/STO SLs. On the other hand, in the bilayer NGO/STO/CCO ($\text{TiO}_2\text{-SrO-CuO}_2$) there is no space for ‘extra’ oxygen ions, since the SrO plane at the interface with the CuO_2 plane is already stoichiometrically full of oxygen ions (figure 7(c)), and no hole doping can occur.

For direct experimental evidence of this finding, scanning transmission electron microscopy (STEM) and electron energy loss spectroscopy (EELS) measurements were performed on both kinds of interfaces [16].

The STEM images of the CCO/STO interface in $(\text{CCO})_9/(\text{STO})_{55}$ bilayer ($\text{CuO}_2\text{-Ca-TiO}_2$ interface) is shown

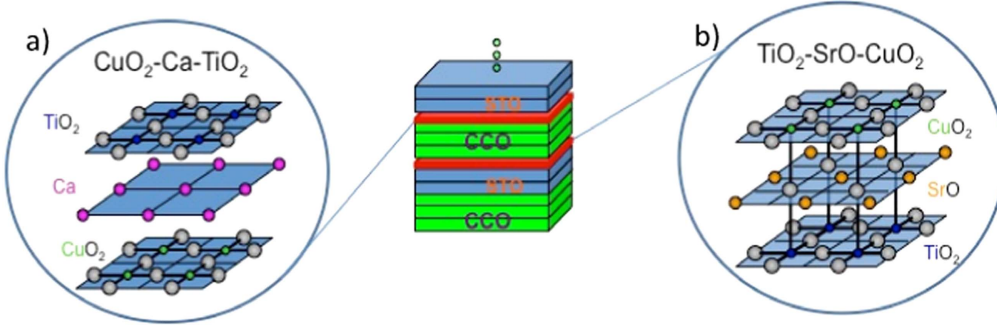


Figure 6. Schematic representation of the two possible interfaces in a CCO/STO superlattice. [30] 2015 © Springer International Publishing Switzerland 2015. With permission of Springer.

in figure 8. Figure 8(c) represents an overlay of the high angle annular dark field (HAADF) image colored in red and the inverted annular bright-field (ABF) image colored in green. In this way, both cations (yellow/orange) and oxygen (green) columns are clearly visible.

From the intensity profiles shown in (d)–(f), taken at the first, second and fourth Ca planes, respectively, in the inverted ABF image (atoms are shown as bright spots on a dark background) it is possible to see that a substantial amount of O ions are present only in the first Ca plane, which thus plays the role of charge reservoir.

The same measurements were also carried out at the STO/CCO interface ($\text{TiO}_2\text{-SrO-CuO}_2\text{-Ca}$) on the trilayer NGO/STO/CCO/STO [16]. They show that all the stoichiometric oxygen ions are present in the interface SrO plane, and that in the Ca plane just above, no oxygen ions are present, so that this interface cannot act as charge reservoir.

The oxygen ions introduced in the interface Ca plane are actually situated in the apical position for the Cu ions belonging to the CuO_2 plane, as already suggested by the study of the SLs. Each oxygen ion provides two holes to the CuO_2 planes. The dependence of the holes' concentration on the distance from the charge reservoir interface has been studied by oxygen (O) K-edge EELS measurements on some bilayers and trilayers. Indeed, it was shown [34–37] that in O K-edge EELS and XAS spectra a pre-edge feature appears when the HTS are doped. O K-edge spectra have been acquired from one interface to the other in sub-angstrom steps. Three sample spectra, taken in the trilayer NGO/STO/CCO/STO, at the STO layer, close to the STO/CCO interface and close to the CCO/STO interface, are shown in panels (a), (b) and (c) of figure 9, respectively.

In the STO layer, which is insulating, no pre-edge feature is observed. On the other hand, in the CCO layer, an additional spectral feature at around 529 eV, named A, appears in the vicinity of the CCO/STO interface and gradually disappears by going towards the STO/CCO interface. This feature, ascribed to delocalized doping holes, is indeed absent far from the CCO/STO interface (figure 3(c)) and in the XAS and EELS spectra of all the insulating cuprates [34–37].

The amplitude of peak A is a measure of the holes' concentration [16, 34–37]. Its behavior as a function of the distance d from the CCO/STO interface is reported in panel (f) of figure 9. The amplitude quickly decays with d roughly as $1/d$, so that in the second CuO_2 plane it is already largely

suppressed. This spatial dependence is associated with the screening of the electrostatic field [38] due to the presence of the excess negatively charged apical oxygen ions within the Ca interface plane.

The conclusion is that only the first CuO_2 plane is substantially doped, the second is slightly doped, and the inner planes are almost undoped.

This result is extremely important, from several aspects. First of all, we can look back to the CCO/STO superlattices, where we know that only one of the two interfaces is doped. Moreover, the doping is confined to the first one or two CuO_2 planes. So, by increasing the number n of CCO unit cells in the SLs, the separation between conducting CCO/STO interfaces increases, although the thickness of the STO separator is kept constant. Therefore, the interaction between conducting CuO_2 planes belonging to different CCO blocks (*interlayer interaction*) decreases. The decrease of the interlayer coupling could be at the root of the T_c decrease in SLs with $n > 3\text{--}4$ unit cells (see figure 5). On the other hand, in the bilayer CCO/STO there is only one isolated interface and no interaction is present. The maximum T_c for the bilayer is about 38 K [16], whereas for the SLs it is about 50 K [27]; the introduction of interlayer interaction in the SLs leads to an increase in T_c of about 25%.

The effect of interlayer interaction can also be revealed by measurements of the superconducting anisotropy γ , defined as $\gamma = (dH_{c2}^{ab}/dt)/(dH_{c2}^c/dt)$, where H_{c2}^{ab} and H_{c2}^c are the upper critical fields along the $a\text{-}b$ plane (the plane of the substrate) and the c -axis (perpendicular to the substrate surface), respectively. The resistance as a function of temperature in different magnetic field has been measured in CCO/STO SLs [39] and a CCO/STO bilayer [40]. The results, reported in figure 10, show that the superconducting anisotropy is about three to four times larger in a CCO/STO bilayer ($\gamma \approx 17\text{--}18$), where there is no interlayer interaction, than in CCO/STO SLs ($\gamma \approx 5\text{--}7$). Thus, the interlayer coupling in the CCO/STO SLs reduces the anisotropy value, as expected.

The other important aspect of this study is related to the similarity between the CCO/STO interface and the native IL/CR interfaces in HTS. This similarity is corroborated by the impressively analogous behavior of T_c as a function of the number of CuO_2 planes in CCO/STO superlattices and in HTS [33]. Moreover, the superconducting anisotropy values of $(\text{CCO})_n/(\text{STO})_m$ superlattices, as shown above, are comparable to that observed in some HTS, such as $\text{YBa}_2\text{Cu}_3\text{O}_x$.

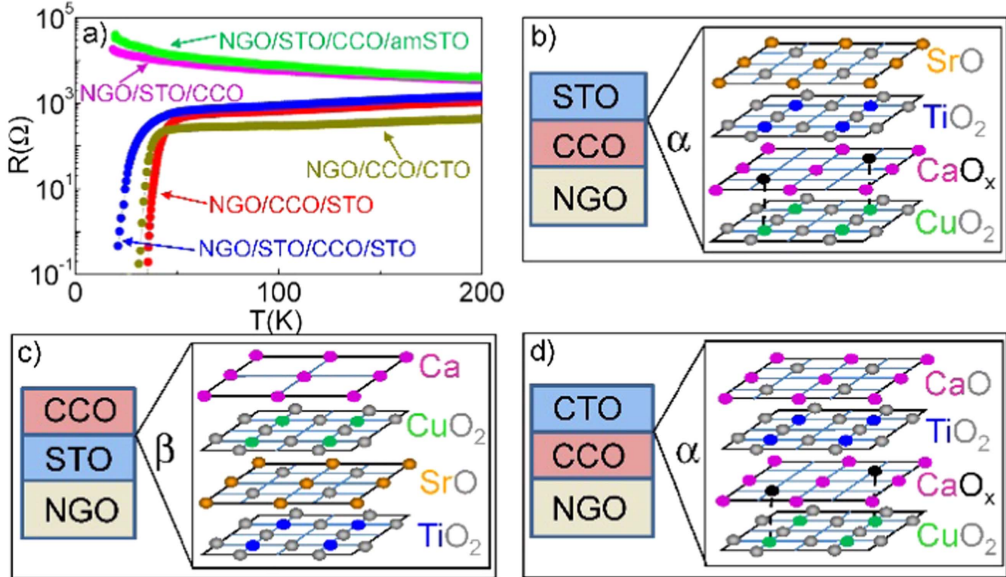


Figure 7. (a) $R(T)$ for $\text{NGO}/(\text{CCO})_{40}/(\text{STO})_{30}$, $\text{NGO}/(\text{CCO})_{40}/(\text{CTO})_{30}$, $\text{NGO}/(\text{STO})_{10}/(\text{CCO})_{40}$, $\text{NGO}/(\text{STO})_{10}/(\text{CCO})_{40}/(\text{STO})_{30}$ and $\text{NGO}/(\text{STO})_{10}/(\text{CCO})_{40}/(\text{STO})_{\text{am}}$ with the top amorphous STO (STO)_{am} layer. (b)–(d) Schematic interface structures for the bilayers $\text{NGO}/\text{CCO}/\text{STO}$ (b), $\text{NGO}/\text{STO}/\text{CCO}$ (c) and $\text{NGO}/\text{CCO}/\text{CTO}$ (d). The extra oxygen ions introduced in the Ca plane at the interface in $\text{NGO}/\text{CCO}/\text{STO}$ and $\text{NGO}/\text{CCO}/\text{CTO}$ are shown in black, together with the corresponding apical coordination with the Cu ions (dashed black line). Reprinted figure with permission from [16], Copyright 2015 by the American Physical Society.

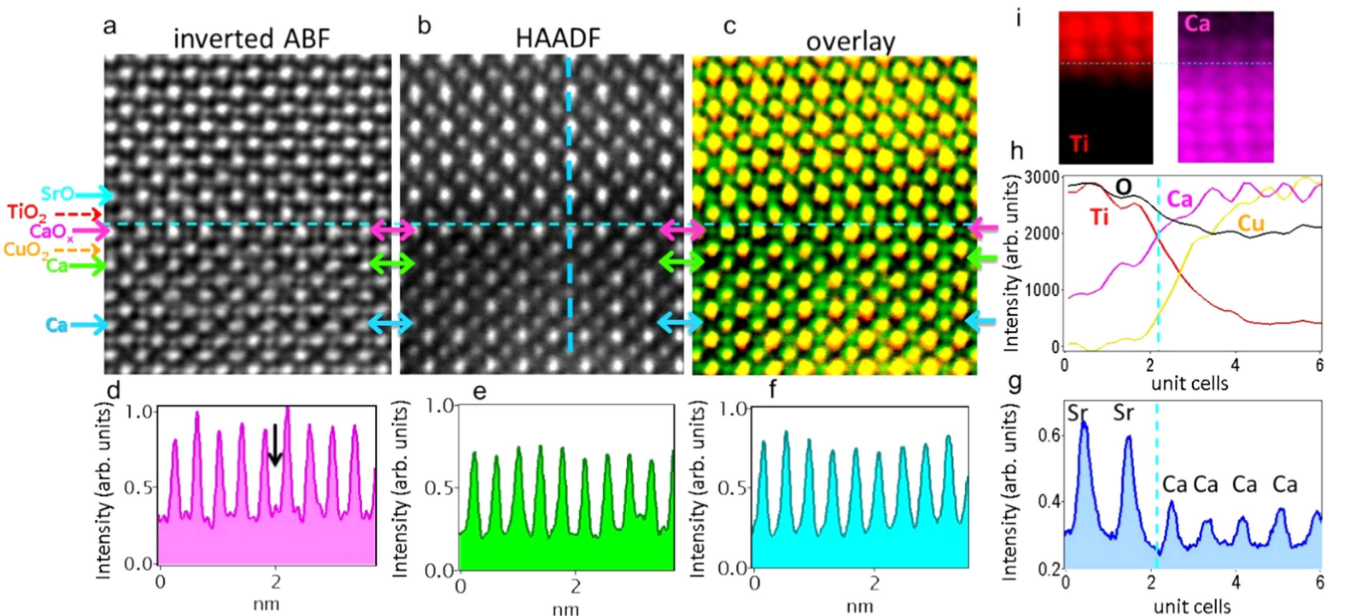


Figure 8. Structure of CCO/STO interface in $\text{NGO}/\text{CCO}/\text{STO}$ bilayer. (a) Inverted ABF images showing O columns. (b) HAADF image showing cations with Z contrast. (c) Overlay of (a) in green and (b) in red, showing all the cations in orange and the O columns in green. (d), (e), and (f) Line profiles of the inverted ABF image at the magenta (interface Ca plane), green and blue arrows, respectively. The black arrow in (d) indicates the intensity from oxygen columns in the interfacial CaO_x plane. (h) EELS elemental profiles. (g) Intensity profile of the HAADF image (taken from the dashed blue line in (b)). (i) EELS elemental maps for Ti and Ca. Dashed cyan lines indicate the interface. Reprinted figure with permission from [16], Copyright 2015 by the American Physical Society.

These indications allow us to conclude that in HTS the dependence of the hole concentration on the distance from the IL/CR interface should be similar to the one found in CCO/STO bilayers (figure 9). The difference is that, in HTS, the two interfaces between IL and CR (CR/IL and IL/CR)

blocks are identical and both are doped, whereas in CCO/STO SLs, only one of the two interfaces is doped. For example, in the $n = 3$ HTS at least two of the three CuO_2 planes are substantially and homogeneously doped. Therefore, in HTS, apart from the *interlayer* interaction among

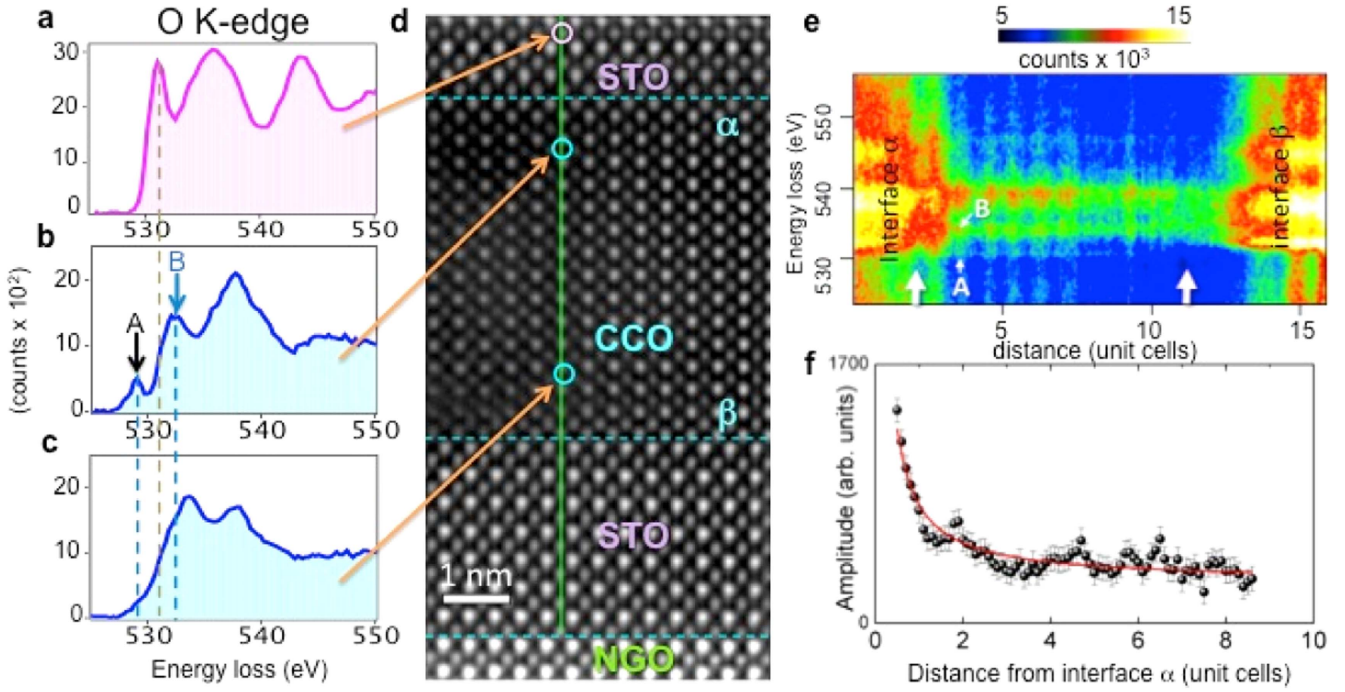


Figure 9. O K-edge measurements in the trilayer NGO/STO/CCO/STO. (a) O K-edge from the upper STO layer in (d). (b) O K-edge from the CCO close to interface α (CCO/STO). (c) CCO O K-edge close to interface β (STO/CCO). (d) HAADF image of the trilayer from which the spectrum image in (e) was taken. (e) Spectrum image (raw data) showing decreasing peak A amplitude in going from interface α to interface β (the big white arrows indicate the range of data shown in (f); the small white arrows indicate the position of peak A and B as indicated in (b)). (f) Amplitude of A as a function of the distance d from the α interface. The line is a fit with $1/d$ dependence. Reprinted figure with permission from [16], Copyright 2015 by the American Physical Society.

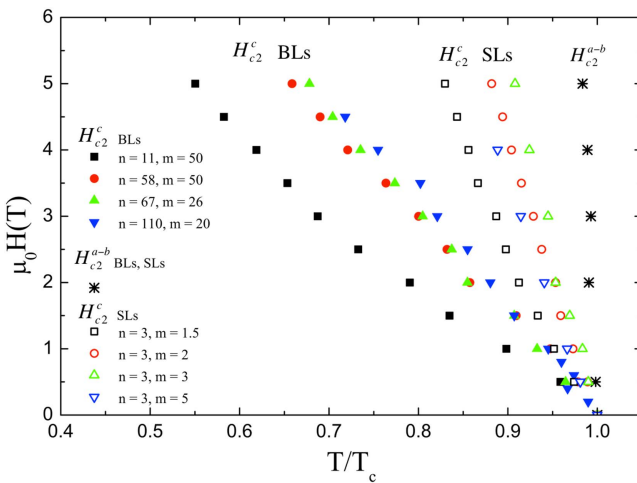


Figure 10. Parallel (stars) and perpendicular (closed symbols) temperature dependence of the upper critical field for all the analyzed bilayers (BLs). Also shown, for comparison, are the perpendicular upper critical fields measured for the superlattices (SLs) (open symbols). The graph legend is specific for BL. Reproduced from [40]. © IOP Publishing Ltd. All rights reserved.

different IL blocks (which is generally almost negligible because of the thickness of the CR block), a sort of interaction among superconducting CuO₂ planes within the same IL block (*intralayer* interaction) is also expected. The latter is absent in CCO/STO SLs, and this fact is probably one of the reasons for the higher critical temperature of the HTS with

$n \geq 2$ (which could be as high as 110 K in $n = 3$ Bi2223, for example) with respect to the CCO/STO SLs.

3. CaCuO₂/BaCuO₂

The presence of two conducting interfaces, analogous to HTS, can be found in another kind of artificial heterostructure, the CaCuO₂/BaCuO₂.

This system consists of two heteroepitaxial blocks: CCO (as for the CCO/STO system) and BaCuO₂ (BCO) in the infinite layer phase (CuO₂ planes separated by bare Ba planes) instead of SrTiO₃. The CCO/BCO system was investigated [12] before the CCO/STO system. However, in this review the order between CCO/STO and CCO/BCO has been reversed for the sake of clarity. Namely, in discussing the CCO/BCO system, we will take advantage of some of the results on CCO/STO obtained by more advanced characterization techniques that were not available at the time the CCO/BCO system was under investigation.

BaCuO₂ in the infinite layer phase is strongly unstable and can easily decompose, forming Ba carbonates. It can be grown as a thin film only because of the pseudomorphic stabilizing effect of a matched substrate such as SrTiO₃, provided that the film thickness does not exceed 30 nm [41]. The BCO system easily incorporates extra oxygen within the Ba plane, giving rise to a metallic behavior. The resistivity of the BCO layer alone is shown in figure 11: it follows a metallic behavior with a moderate slope at high temperature and turns to a

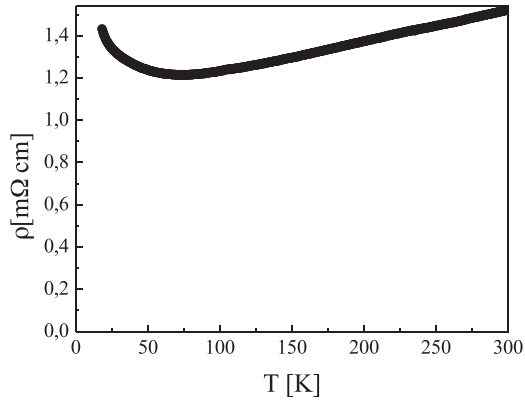


Figure 11. Behavior of resistivity vs temperature for a BCO film about 10 nm thick grown on a NdGaO₃ (110) substrate.

semiconducting-like behavior below 100 K. No trace of superconductivity is detected even for strongly oxidized samples.

The lack of superconductivity in the BCO structure was attributed to the high degree of structural disorder that involves the CuO₂ planes in the BCO structure [42], which actually loses its pure infinite layer character. Indeed, whereas the Ba planes incorporate extra oxygen ions, a lack of oxygen ions occurs in the CuO₂ planes [42], inducing a disorder detrimental for superconductivity. On the other hand, it was shown that if a [(CCO)_n/(BCO)_m]_N superlattice is deposited in strongly oxidizing conditions, the Ba planes in the BCO block include excess oxygen ions, while the CCO block remains in the ideal infinite layers structure. Consequently, the interface Ba layer acts as a charge reservoir for the CCO block, giving rise to superconductivity. Figure 12 shows a sketch of the CCO/BCO superlattice structure. In some cases, in order to increase the stability of the Ba-based IL structure, Ba was partially substituted by Nd, resulting in the chemical composition Ba_{0.9}Nd_{0.1}CuO_{2+x}. Hereafter, both Ba_{0.9}Nd_{0.1}CuO_{2+x} and BaCuO_{2+x} compounds will be indicated as BCO.

The behavior of resistance versus temperature was measured for a large number of (CCO)_n/(BCO)₂ superlattices grown in identical experimental conditions but having CCO layers of different thicknesses, whereas the thickness of the BCO block was kept constant at $m = 2$ (as for CCO/STO SLs).

In this structure, extra oxygen ions in the Ba planes are only partially compensated by oxygen vacancies in the CuO₂ planes [42]. Overall, there is an excess of oxygen ions in the interface Ba plane. In turn, this plane is able to dope by holes the next neighbor CuO₂ plane in the IL block, giving rise to superconductivity, which is analogous to what happens in the CCO/STO system. An important difference relative to the CCO/STO system is that the bottom and top interfaces (see the sketch of the structure in figure 12) are identical and contain Cu atoms in tetrahedral coordination. Therefore, both interfaces are expected to be hole-doped and superconducting. Consequently, in the case of the CCO/BCO system, beside the *interlayer* interaction, already discussed in connection with the CCO/STO system, the interaction between superconducting layers belonging to the same CCO block must also be considered. We refer to this

coupling as an *intralayer* interaction. In figure 12 we report the T_c as a function of the number of CuO₂ sheets, n_{CuO_2} , for a large number of superlattices with different thicknesses of the CCO block (n CCO unit cells) but the same BCO block thickness ($m = 2$ BaCuO_{2+x} unit cells), grown in the same conditions. According to figure 12, T_c versus n_{CuO_2} follows qualitatively the same behavior as for the CCO/STO SLs, with a maximum T_c occurring between three and four CuO₂ sheets, but with a higher value of maximum T_c (above 80 K). The dependence of T_c on n_{CuO_2} is similar to the conventional HTS compounds. T_c strongly depends on n_{CuO_2} : the maximum value of T_c is above 80 K, while T_c is reduced to about 30 K for $n_{\text{CuO}_2} = 7$. The decrease of T_c for large n_{CuO_2} values cannot be ascribed to the dilution of the doping holes over the whole thickness of the IL block, because the holes essentially remain confined in the CuO₂ plane nearest neighbor to the doping interface, as we have seen from EELS measurements on the CCO/STO system (see previous section).

Successively, based on the idea that each IL block contains two superconducting sheets (corresponding to the two opposite interfaces with the BCO layers), we have grown a thin heterostructure consisting of $n = 2$ CaCuO₂ unit cells sandwiched between $m = 5$ BCO layers (a 5/2/5 heterostructure). Moreover, the resistivity behavior of a superlattice consisting of $m = 5$ BCO unit cells and $n = 2$ CaCuO₂ unit cells (5 × 2 SL) was measured for comparison. Figure 13 shows the comparison between the two samples. The transition temperature is about the same (about 60 K), which is roughly 20 degrees lower than the best 2 × 2 superlattice (figure 12). In these samples, each CCO block contains two superconducting interface CuO₂ sheets spaced by 6.4 Å (two CaCuO₂ unit cells). Furthermore, in the case of the superlattice, each superconducting sheet is separated by five unit cells of BaCuO_{2+x} (~20 Å) from the nearest neighbor superconducting sheet in the adjacent CCO block. We notice that in the 5/2/5 heterostructure no interlayer interaction can occur, as this sample contains a single CCO block made by two CCO unit cells. The circumstance that the critical temperature has the same value for the two samples indicates that in the 5 × 2 SL the interlayer interaction between the superconducting sheets in adjacent CCO blocks separated by a BCO block is weak, at least for such large values of the spacing ($m = 5$) between nearest neighbor CCO blocks.

However, comparing the T_c for the 5 × 2 SL with the value reported in figure 12 for the 2 × 2 SL (corresponding to three CuO₂ sheets), we are led to conclude that the interlayer coupling can contribute to the strengthening of the superconducting interaction when the distance between next neighbor CCO blocks is reduced to only two BaCuO_{2+x} unit cells. The percentage increase in T_c due to the interlayer interaction (from about 60 K to about 80 K) is about 25%, which is in agreement with the values found for the CCO/STO superlattices (see previous section).

Magnetoresistance measurements in a perpendicular magnetic field were carried out on 2 × 2 and 5 × 2 SLs, as well as on a 5/2/5 heterostructure. The results reinforce the above reported conclusions concerning the interlayer interaction. Namely, figure 14 shows that the broadening of the transition in the magnetic field, related to the superconducting anisotropy of the system, is roughly the same for the 5 × 2 SL and the 5/2/5 heterostructure. Conversely, the anisotropy for the 2 × 2 SL is

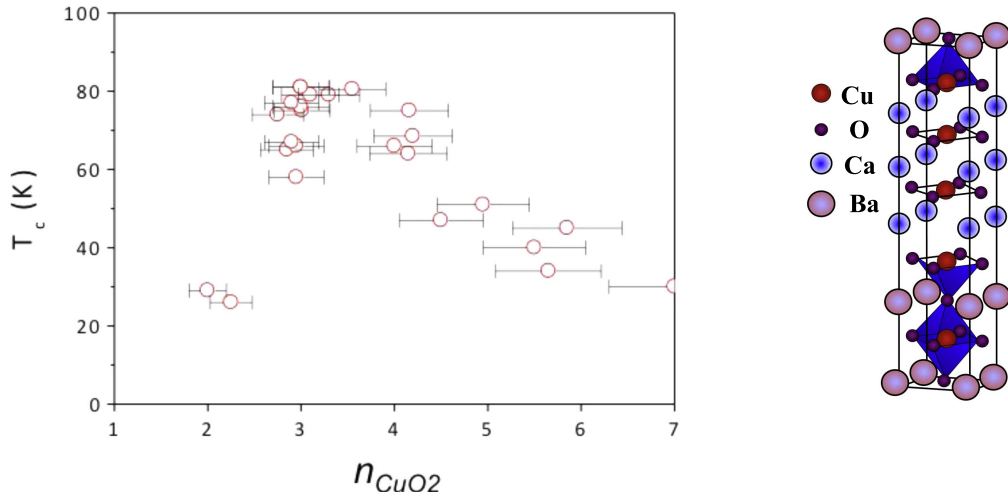


Figure 12. Left panel: behavior of T_c versus n_{CuO_2} , the number of CuO_2 sheets between two BCO blocks, in $(\text{CCO})_n/\text{BCO}_2$ SLs. Right panel: schematics of the superlattice structure for $(\text{CCO})_n/\text{BCO}_2$ with $n = 3$ (i.e. $n_{\text{CuO}_2} = 4$ CuO_2 sheets).

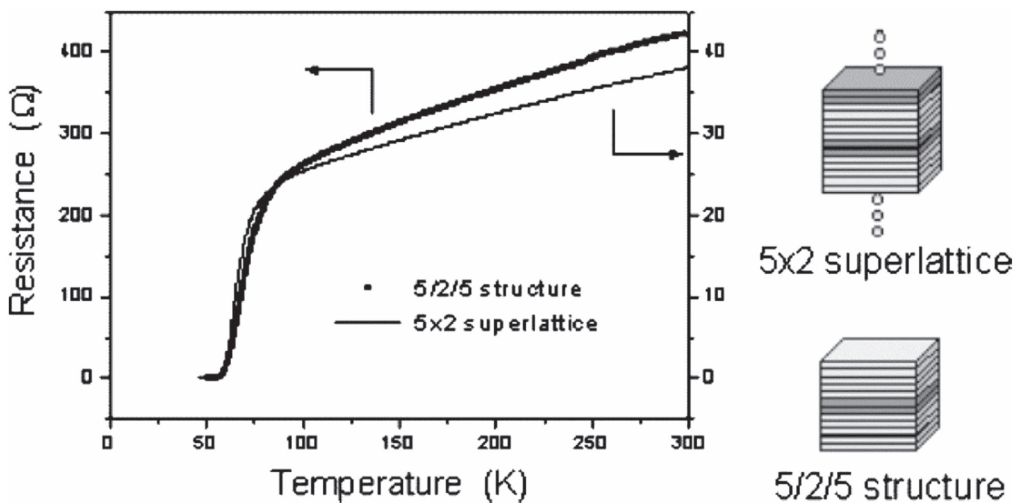


Figure 13. Resistance versus temperature behavior of a CCO/BCO with $n = 2$ and $m = 5$ (5×2 superlattice) and of a $5/2/5$ structure is shown. A rough sketch of the two structures is shown on the right-hand side. Reprinted from [43], with the permission of AIP Publishing.

much lower, since in this case a coupling between adjacent CCO layers is present via the interlayer interaction. The other two cases (5×2 SL and $5/2/5$ heterostructure) are similar, since the thickness of the BCO block in the 5×2 superlattice is large enough to prevent substantial interlayer interaction. Therefore, in this respect, there is no difference between the 5×2 SL and the $5/2/5$ heterostructure, as also shown by their identical T_c .

A simple analysis of the data reported in figure 14, based on [45], leads to estimates for the anisotropy factor γ of about 20 and 50 for the 2×2 SL and the 5×2 SL, respectively [44]. In the former sample both the intralayer and the interlayer interactions are active, while in the latter case, because of the large separation (five BCO unit cells) between the adjacent IL blocks, the interlayer interaction can be neglected. The values quoted above are intermediate, in between those typical of YBCO and those typical of BSCCO.

Successively, in order to investigate the properties of an individual superconducting interface, we have grown a

heterostructure consisting of a CCO layer grown on a BCO layer. The heterostructure was capped with a protective layer, consisting of amorphous CCO deposited at low temperature. The inset of figure 15 shows a sketch of this heterostructure. The amorphous cap layer is not expected to lead to a superconducting interface with the underlying monocrystalline CCO. Therefore, a single superconducting 2D layer occurs at the interface between BCO and CCO, showing that for the CCO/BCO system, as for the CCO/STO system, interlayer and intralayer interactions are not necessary for superconductivity.

Moreover, no relevant dependence of the transition temperature on the CR block thickness was found (figure 15). This result shows that hole doping of the CaCuO_2 layer is not affected by the overall oxygen excess, which is expected to increase with the thickness of the CR block. Therefore, we argue that, in an analogy with the case of CCO/STO, doping of the CCO layer can be ascribed to the single BaO_x plane at the interface with the CCO block and not to charge transfer from the bulk of the BCO

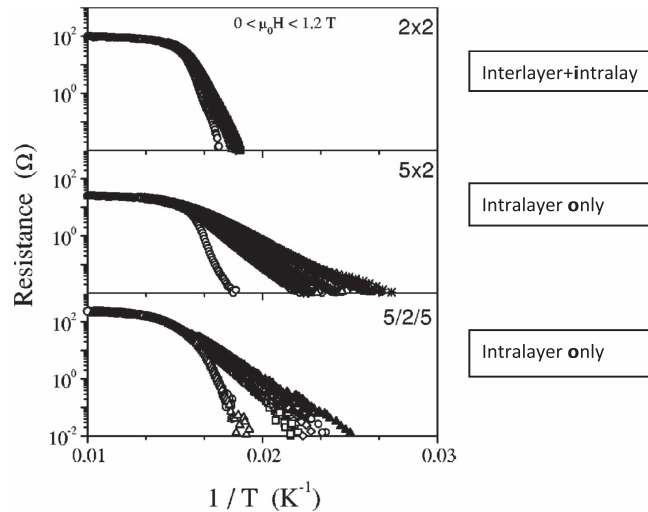


Figure 14. Magnetoresistance of 2×2 and 5×2 superlattices and $5/2/5$ heterostructure, with the magnetic field ($0 < \mu_0 H < 1.2$ T) perpendicular to the CuO_2 planes, shown in an Arrhenius plot. Reprinted figure with permission from [44], Copyright 2001 by the American Physical Society.

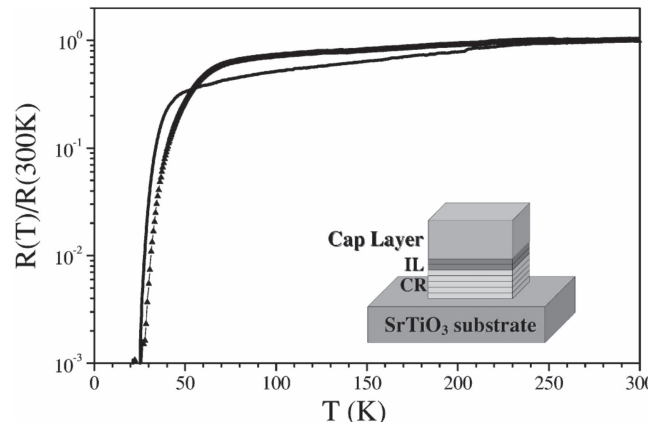


Figure 15. Resistance (normalized to the 300 K value) behavior of the $(\text{Ba}_{0.9}\text{Nd}_{0.1}\text{CuO}_{2-x})_m/(\text{CaCuO}_2)_2$ artificial structure with $m = 2$ (full line) and $m = 5$ (triangles). In the inset the m/n structure is schematically sketched. Reprinted figure with permission from [46], Copyright 2002 by the American Physical Society.

CR block. Samples of figure 15 represent the simplest superconducting structure, with a single 2D superconducting layer and without intralayer or interlayer interaction with adjacent superconducting layers. It is also worth noticing that the T_C of this structure is slightly lower (about 5 K lower) than the T_C for the 2×7 superlattice where the two BCO/CCO interfaces are far apart (seven unit cells of CCO) and no sizeable intralayer interaction is expected.

4. $\text{La}_2\text{CuO}_4/\text{La}_{2-x}\text{Sr}_x\text{CuO}_4$

Gozar *et al* used a different approach to the study of the interface superconductivity in cuprates [13]. They grew epitaxial heterostructures consisting of metallic (non-superconducting) $\text{La}_{2-x}\text{Sr}_x\text{CuO}_4$ (LSCO) and the undoped insulating parent

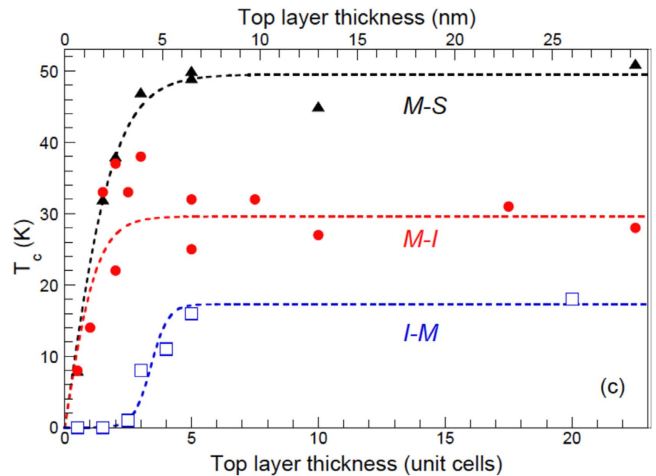


Figure 16. Dependence of T_C on the top layer thickness in I–M, M–I. Also the T_C for metal/superconductor (M–S) bilayers are shown in the figure, but not discussed in the text. The critical temperature is taken as the midpoint of the resistive transition. Reprinted by permission from Macmillan Publishers Ltd: Nature [13], Copyright 2008.

compound La_2CuO_4 (LCO). The stacking sequence of the La_2CuO_4 phase consists of a single CuO_2 plane separated by two LaO planes with the rock salt (CR) structure. The transport properties in these compounds may span the full range from an insulating behavior to superconducting and, finally, to metallic (non-superconducting) behavior, as the doping level varies. In practice, in LCO doping is achieved either by forcing excess oxygen ions into the structure or by substituting divalent Sr for trivalent La. The critical temperature depends on the hole doping: below 0.06 holes per formula unit, LSCO is an insulator; between 0.06 and 0.2 it shows superconductivity; and above 0.2 it is a simple metal.

An epitaxial heterostructure consisting of an overdoped metallic LSCO layer (M) and an insulating undoped LCO layer (I) was grown [13]. In this case, although neither of the layers is individually superconducting, the overall structure shows superconducting properties. In these heterostructures the T_C depends on the stacking sequence, as shown in figure 16. The critical temperature sharply rises as soon as the thickness of the overlayer exceeds two or three unit cells and saturates above five unit cells, similar to CCO/STO SLs (see [26] and figure 5). The resulting saturation value for T_C (here it is taken as the midpoint of the transition) is 15 K for the stacking sequence consisting of LSAO (substrate)–I–M, while it reaches the value of 30 K if the order sequence of I and M is reversed (LSAO–M–I structure), with a maximum of 38 K for three to four cells of the top I layer (see figure 16). Such an effect was attributed to charge redistribution at the interface between the insulating LCO and the metallic LSCO. It must be noted that the same effect, superconductivity at the interface, could be also achieved because of some Sr/La interdiffusion between the two constituent layers. That is to say, interdiffusion would allow decreasing the doping of the metallic layer while increasing at the same time the doping of the insulating layer. This process might result in an optimally doped and superconducting interface layer. However, advanced characterization techniques have shown that interdiffusion is almost negligible and confined to one unit cell at the interface

[47]. Successively, with the aim of localizing the superconducting layer within the heterostructure, the same authors selectively doped the CuO_2 planes by isovalent Zn [48]. Zn doping is known to depress severely T_C . They observed that the T_C of the heterostructure is depressed only when Zn selectively dopes the CuO_2 plane's second-closest neighbor to the interface on the side of LCO. Overall, it was concluded that superconductivity in the bilayer takes its origin from charge transfer from the LSCO metallic layer into the LCO insulating layer and is confined in a single La_2CuO_4 unit cell.

This heterostructure is thus similar to the bilayer made by CCO/STO and BCO/CCO illustrated in the previous sections, with only one isolated superconducting CuO_2 plane at the interface, and without inter- and intralayer interaction. The resulting T_C of this heterostructure is indeed very similar to the other two cases ($T_C \approx 38$ K in the CCO/STO bilayer and $T_C \approx 25$ K in the CCO/BCO bilayer).

5. Discussion

Experimental data concerning superlattices and interfaces discussed in the former section suggest that high T_C superconductivity in cuprates is, by nature, a 2D phenomenon, and interaction among different superconducting layers is not strictly required in order to achieve superconductivity. In fact, interaction among different superconducting 2D layers results in an increase of the critical temperature and a decrease of the anisotropy. Interaction between superconducting layers can involve layers within the same IL block and layers belonging to adjacent IL blocks; in the former case, we referred to the interaction as an *interlayer* interaction, and in the latter case as an *intralayer* interaction. By using different heterostructures we are able to separate the different contributions. In practice, experiments carried out on three different cuprate systems (CCO/STO, CCO/BCO and LSCO/LCO) and on LAO/STO have shown that superconductivity can manifest itself as purely an interface effect. In the case of cuprate-based heterostructures, the transition temperature of a single isolated interface depends critically on the growth conditions, and especially on the sample oxidation conditions. In the best cases a transition temperature of 38 K (zero resistance point), 25 K (zero resistance point) and 38 K (midpoint) were measured for CCO/STO, CCO/BCO and LSCO/LCO, respectively. The moderate differences among the T_C values appear to be real. In this respect, a comparison can be made with standard HTS compounds containing a single CuO_2 plane and, therefore, no intralayer interaction and a negligible interlayer interaction (given the thickness of the CR block). The T_C values are roughly in the same temperature range for Bi2201 (20 K) and LCO (40 K), but they are definitely larger in a $\text{Tl}_2\text{Ba}_2\text{CuO}_6$ compound with $n = 1$ (80 K) and in $\text{HgBa}_2\text{CuO}_4$ with $n = 1$ (94 K). This result proves that T_C is not a universal property of the CuO_2 plane at the interface, but rather that it depends on the structural and chemical details of the interface itself. The large spread in T_C values shows that the interface structure is the major ingredient that rules the transition temperature in HTS. Similar considerations hold for

the anisotropy of the superconducting properties. The anisotropy of a single superconducting layer at the CCO/STO interface has a value that compares well with values found for standard HTS compounds. Switching on interlayer and intralayer interactions results in a moderate decrease of the anisotropy. In other words, this implies that anisotropy too is mostly an intrinsic property of the interface that depends on the structural and chemical details of the interface itself.

We discuss now the role of the interlayer and of the intralayer interactions on the superconducting transition temperature. We take advantage of the circumstance that in the CCO/STO heterostructures only the $\text{CuO}_2\text{--CaO}\text{--TiO}_2$ interface is hole-doped and superconducting, while the $\text{TiO}_2\text{--SrO}\text{--CuO}_2$ is not. On the contrary, in the CCO/BCO heterostructures both interfaces are superconducting. The situation is schematically described in figure 17, which shows a sketch of a $n = 3, m = 2$ (3×2) CCO/STO superlattice and a $n = 3, m = 2$ (3×2) CCO/BCO superlattice. The hole-doped and superconducting CuO_2 planes are shadowed in red. A remarkable difference can be noticed between the two superlattices. For the CCO/STO superlattice, a single superconducting layer occurs within a CCO block. In this case, doping originates from the extra oxygen ions in the Ca plane faced to the topmost TiO_2 plane of the STO block. Holes are induced in the next neighbor CuO_2 plane belonging to the CCO block. According to the STEM-EELS measurements discussed previously, holes spread out over only a very thin layer in the CCO block [16]. The upper interface between CCO and STO is not doped by the SrO plane and, therefore, is not superconducting.

The situation for the CCO/BCO superlattices is different. In this case, doping oxygen ions accumulate more easily in the Ba planes, and holes spread over the nearest neighbor CuO_2 plane that belongs to the CCO block. The same mechanism holds for both the interfaces (see figure). The circumstance that the single BCO film grown under strongly oxidizing conditions (and therefore heavily oxygen-doped) is never superconducting leads to the conclusion that the CuO_2 planes encompassed between two Ba planes are not superconducting. Overall, the major result of the above discussion is that for CCO/STO, a single superconducting layer occurs per CCO block and, therefore, only interlayer interaction is possible. Conversely, for CCO/BCO, two superconducting interface layers occur per CCO block, resulting in an additional intralayer interaction.

Therefore, in the CCO/STO system the intralayer interaction does not play a role, while the interlayer interaction can be tuned by changing the thickness of the CCO/STO bilayer that separates two adjacent superconducting sheets. Conversely, for the CCO/BCO system, intralayer and interlayer interactions can be modulated separately by varying the thicknesses of the CCO block and the BCO block, respectively. Figure 18 reports the T_C of CCO/BCO (green dots) as a function of two phenomenological parameters: 'strength of the interlayer interaction' (ITE) and 'strength of the intralayer interaction' (ITR). Assuming that the intralayer interaction is simply proportional to the reciprocal of the thickness of the CCO block that separates the two superconducting interface sheets, we define the ITR for the CCO/BCO system as the reciprocal of the number n of CCO unit cells in the CCO

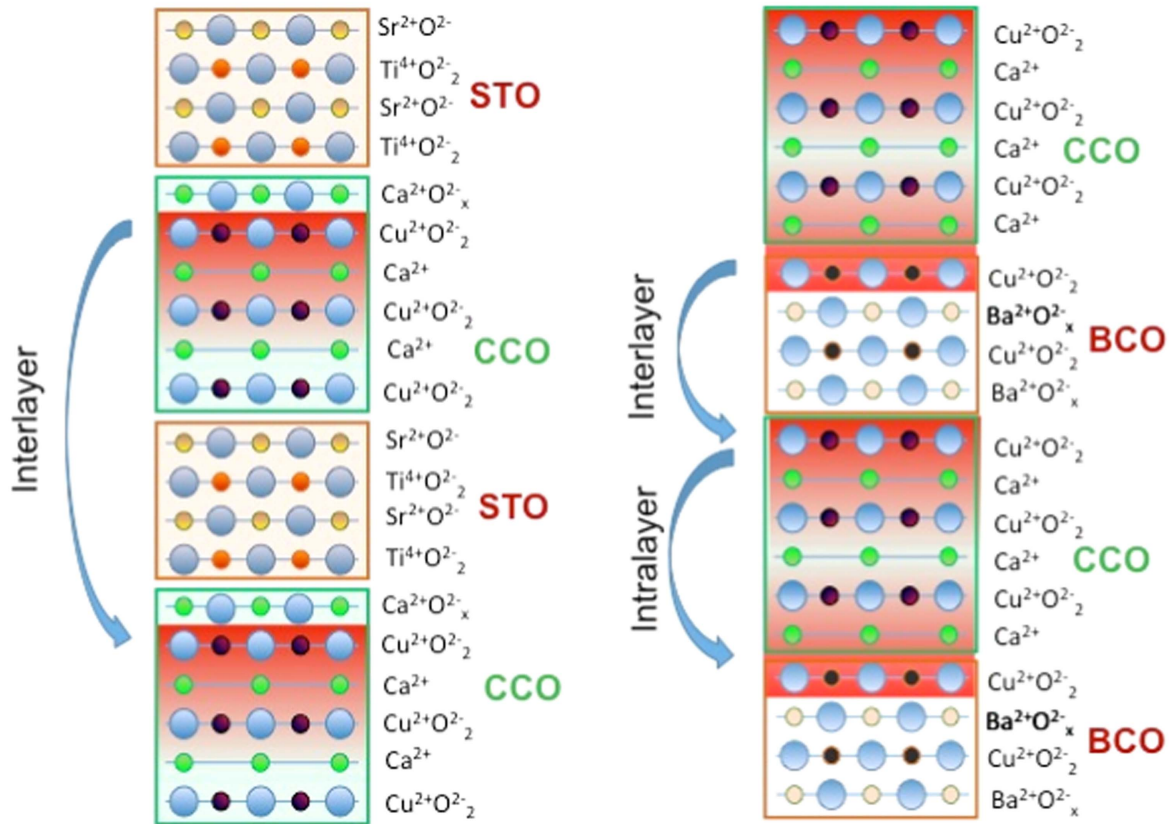


Figure 17. Sketch of a 3×2 CCO/STO superlattice and a 3×2 CCO/BCO superlattice. The hole-doped and superconducting CuO_2 planes are shadowed in red. For the CCO/STO superlattice, a single superconducting layer occurs within a CCO block, while two superconducting layers are present in the CCO/BCO superlattice. Intralayer and interlayer interactions are indicated.

block. (No definition is needed in CCO/STO for this interaction.) Analogously, the ITE is defined as the reciprocal of the BCO block thickness m measured in BaCuO_2 unit cells. A zero interlayer and zero intralayer interaction characterize the ideal single interface. Figure 18 shows that, at a constant $\text{ITE} = 0.5$, the critical temperature increases with increasing ITR to a maximum value that occurs at $\text{ITR} = 0.33$. Above this value (that is, for a smaller n), the T_C decreases in accordance with the standard behavior of the HTS compounds. Relative to the pure interface value (zero ITE and zero ITR), T_C increases by a factor of two to three (from about 25 to about 60 K) by adding the intralayer interaction alone. In comparison, the dependence of the critical temperature of CCO/BCO on ITE is weaker; it leads, for a constant ITR = 0.5, to an increase of about 20% (from 60 K to 70 K).

Together with the data for the CCO/BCO system, we also report in figure 18 the experimental data for the CCO/STO system (red dots). In these SLs there is no intralayer interaction. Therefore, all representative points lie in a single plane corresponding to zero ITR. For a $[(\text{CaCuO}_2)_n/(\text{SrTiO}_3)_m]_N$ superlattice, the interlayer strength is defined as $1/(n+m)$. Figure 18 shows the effect of the interlayer interaction on T_C : decreasing the separation between superconducting layers, T_C first slightly increases and then decreases when the thickness of the individual layers becomes smaller than a couple of unit cells (possibly because of interface roughness effects). The percentage increase of T_C due to the interlayer interaction is

similar to the CCO/BCO system, as it goes from 38 K in the bilayer with $\text{ITE} = 0$, to about 50 K in the SL with $\text{ITE} \approx 0.2$ (about a 25% increase).

6. Conclusions

The full set of data illustrated in the present review allows the drawing of some interesting conclusions that, very likely, also hold in the case of standard high temperature superconducting cuprates.

The most relevant result is that a single interface between two oxides can support superconductivity with a high critical temperature and only a moderate anisotropy. The T_C value and the anisotropy of a single interface is very much sample-dependent: in CCO/STO the T_C of a single interface is about 38 K, whereas in CCO/BCO it is about 25 K. If we look at a conventional HTS with $n = 1$, we have that in LCO the $T_C = 40$ K, in Bi-compound the $T_C = 20$ K, in Tl-compound the $T_C = 80$ K and in Hg-compound the $T_C = 94$ K. So the T_C of the isolated interface depends, possibly, on structural and chemical details of the interface itself, as previously suggested for HTS [49].

In a superlattice structure, the interaction with other superconducting interfaces can increase the T_C and reduce the anisotropy. Two different interactions can be envisaged: *intralayer* (within the same active block) and *interlayer*

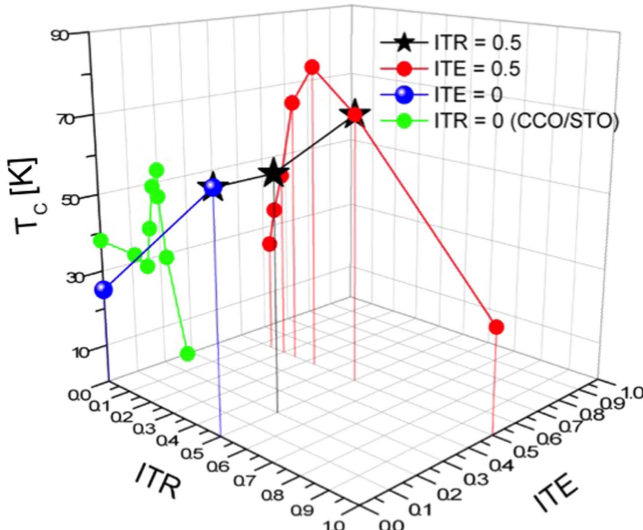


Figure 18. T_c values for different CCO/BCO samples. The red dots correspond to the T_c measured in CCO/BCO systems with the same ITR and different values of ITE. The black stars correspond to the T_c measured in CCO/BCO systems with the same value of ITR and different ITE. The blue dots have constant ITE = 0 and different values of ITR. The green dots represent the T_c for CCO/STO systems, which all have ITR = 0.

(between adjacent active blocks). Engineering suitable heterostructures has allowed the separation of the two contributions. The intralayer interaction has been shown to be much more effective in increasing the transition temperature and decreasing the anisotropy. This finding is in qualitative agreement with the dependence of the critical temperature on the number n of CuO_2 planes in the IL block for HTS cuprates. The interlayer interaction makes a further moderate contribution to strengthen superconductivity. In this respect it is worth noting that artificial heterostructures offer the possibility of varying independently the intralayer and interlayer interactions, while in standard HTS cuprates they cannot be easily disentangled as they are active together.

A further important result is that hole doping of the CuO_2 planes in the superconducting IL block depends on a single interface plane rather than on the bulk of the ‘charge reservoir’ block. In other words, thickening the charge reservoir block, and thus the overall excess oxygen in the charge reservoir block, does not increase the doping of the superconducting IL block. Furthermore, experimental data shown in the present review demonstrate that the average doping for the CuO_2 plane is not the crucial issue, and it has to be substituted by the concept of the local holes’ concentration at the interface. Namely, the holes’ concentration decreases strongly within very few atomic planes from the doping interface. Therefore, even for a very thick active layer, where the average holes’ concentration for the CuO_2 plane is small, the effective holes’ concentration at the doping interface is essentially unaffected. Extending these conclusions to the standard HTS cuprates, the characteristic ‘bell-shaped’ dependence of the critical temperature on the number n of CuO_2 planes in the IL block cannot be attributed to a change of the hole doping per Cu site, but rather to some kind of intralayer interaction similar to that proposed in [50]. We argue that the T_c

increases strongly when n is increased from 1 to 2 in HTS, since the intralayer interaction is switched on. The further increase occurring when n rises from 2 to 3 can have several explanations, which are beyond the scope of the present review. We just mention that recently it has been pointed out [51] that the presence of apical oxygen tends to localize the holes in the CuO_2 plane. So, when in $n = 3$ HTS, a CuO_2 plane without apical oxygen is introduced in the middle, this is still substantially doped and the T_c increases. With further increasing of n , the ITR and the T_c decrease coherently, according to figure 18.

In conclusion, we believe that the results from the present review may offer a perspective for engineering novel artificial structures having higher critical temperatures and lower anisotropy. The search for doping interfaces should be extended to new systems, possibly with higher intrinsic T_c . The structure should be centrosymmetric, with both interfaces superconducting (as for CCO/BCO). The CCO block should comprise three or four CuO_2 planes to maximize the intralayer interaction and to have apical-free CuO_2 planes, while the CR block should be thin to increase the interlayer interaction. For instance, from the data of figure 18 we can guess that, if an intralayer interaction could be switched on for the CCO/STO system, a T_c well above 80 K should be achieved.

ORCID iDs

Daniele Di Castro <https://orcid.org/0000-0002-0878-6904>
Giuseppe Balestrino <https://orcid.org/0000-0002-6687-6748>

References

- [1] Little W A 1964 *Phys. Rev.* **13** A1416
- [2] Ginzburg V L 1964 *Phys. Lett.* **13** 101
- [3] Drozdov A P, Eremets M I, Troyan I A, Ksenofontov V and Shylin S I 2015 *Nature* **525** 73–6
- [4] Troyan I *et al* 2016 *Science* **351** 1303–6
- [5] Gao L *et al* 1994 *Phys. Rev. B* **50** 4260–3
- [6] Wu G *et al* 2009 *J. Phys.: Condens. Matter* **21** 142203
- [7] Strongin M and Kammerer O 1968 *J. Appl. Phys.* **39** 2509–14
- [8] Khlyustikov I N and Buzdin A I 1987 *Adv. Phys.* **36** 271–330
- [9] Ge J F *et al* 2015 *Nat. Mater.* **14** 285–289A
- [10] Navarro-Moratalla E *et al* 2016 *Nat. Commun.* **7** 11043
- [11] Talantsev E F, Crump W P, Island J O, Xing Y, Sun Y, Wang J and Tallon J L 2017 *2D Mater.* **4** 025072
- [12] Balestrino G *et al* 1998 *Phys. Rev. B* **58** R8925
- [13] Gozar A, Logvenov G, Fitting Kourkoutis L, Bollinger A T, Giannuzzi L A, Muller D A and Božović I 2008 *Nature* **455** 782
- [14] Reyren N *et al* 2007 *Science* **317** 1196
- [15] Biscaras J, Bergeal N, Kushwaha A, Wolf T, Rastogi A, Budhani R C and Lesueur J 2010 *Nat. Comm.* **1** 89
- [16] Di Castro D *et al* 2015 *Phys. Rev. Lett.* **115** 147001
- [17] Bollinger A T and Božović I 2016 *Supercond. Sci. Technol.* **29** 103001
- [18] Wang L, Ma X and Xue Q-K 2016 *Supercond. Sci. Technol.* **29** 123001
- [19] Gariglio S, Gabay M, Mannhart J and Triscone J-M 2015 *Physica C* **514** 189–98
- [20] Ohtomo A and Hwang H Y 2004 *Nature* **427** 423–6
- [21] Tsukazaki A *et al* 2007 *Science* **315** 1388

- [22] Kleibeuker J E *et al* 2014 *Phys. Rev. Lett.* **113** 237402
- [23] Pentcheva R *et al* 2010 *Phys. Rev. Lett.* **104** 166804
- [24] Caviglia A D *et al* 2008 *Nature* **456** 624
- [25] Tanaka Y *et al* 2014 *J. Phys. Soc. Jpn.* **83** 074705
- [26] Di Castro D *et al* 2012 *Phys. Rev. B* **86** 134524
- [27] Di Castro D, Aruta C, Tebano A, Innocenti D, Minola M, Moretti Sala M, Prellier W, Lebedev O I and Balestrino G 2014 *Supercond. Sci. Technol.* **27** 044016
- [28] Siegrist T, Zahurak S M, Murphy D W and Roth S R 1988 *Nature* **334** 231
- [29] Balestrino G, Desfeux R, Martellucci S, Paoletti A, Petrocelli G, Tebano A, Mercey B and Hervieu M 1995 *J. Mater. Chem.* **5** 1879
- [30] Di Castro D and Balestrino G 2015 High Tc superconductivity in engineered cuprate heterostructures *Oxide Thin Films, Multilayers, and Nanocomposites* ed P Mele *et al* (Berlin: Springer) (https://doi.org/10.1007/978-3-319-14478-8_3)
- [31] de Groot F M F, Fuggle J C, Thole B T and Sawatzky G A 1990 *Phys. Rev. B* **41** 928
- [32] Fink J, Nücker N, Pellegrin E, Romberg H, Alexander M and Knupfer M 1994 *Electron Spectrosc. Relat. Phenom.* **66** 395
- [33] Iyo A, Tanaka Y, Kodama Y, Kito H, Tokiwa K and Watanabe T 2006 *Physica C* **445–448** 17–22
- [34] Romberg H, Alexander M, Nucker N, Adelmann P and Fink J 1990 *Phys. Rev. B* **42** 8768
- [35] Gauquelin N, Hawthorn D G, Sawatzky G A, Liang R X, Bonn D A, Hardy W N and Botton G A 2014 *Nat. Commun.* **5** 4275
- [36] Chen C T *et al* 1991 *Phys. Rev. Lett.* **66** 104
- [37] Chen C T, Tjeng L H, Kwo J, Kao H L, Rudolf P, Sette F and Fleming R M 1992 *Phys. Rev. Lett.* **68** 2543
- [38] Kotegawa H 2001 *J. Phys. Chem. Solids* **62** 171
- [39] Salvato M, Ottaviani I, Lucci M, Cirillo M, Di Castro D, Innocenti D, Tebano A and Balestrino G 2013 *J. Phys. Condens. Matter* **25** 335702
- [40] Salvato M, Tieri G, Balestrino G and Di Castro D 2015 *Supercond. Sci. Technol.* **28** 095012
- [41] Maeda T, Yoshimoto M, Shimozono K and Koinuma H 1995 *Physica C* **247** 142
- [42] Colonna S, Arciprete F, Balzarotti A, Balestrino G, Medaglia P G and Petrocelli G 2000 *Physica C* **334** 64
- [43] Balestrino G, Lavanga S, Medaglia P G, Orgiani P, Paoletti A, Pasquini G, Tebano A and Tucciarone A 2001 *Appl. Phys. Lett.* **79** 99
- [44] Balestrino G, Lavanga S, Medaglia P G, Orgiani P and Tebano A 2001 *Phys. Rev. B* **64** 20506
- [45] Tinkham M 1996 *Introduction to Superconductivity* 2nd edn (New York: McGraw-Hill)
- [46] Balestrino G, Lavanga S, Medaglia P G, Orgiani P and Tebano A 2002 *Phys. Rev. B* **66** 094505
- [47] Logvenov G *et al* 2010 *J. Phys. Chem. Solids* **71** 1098
- [48] Logvenov G, Gozar A and Bozovic I 2009 *Science* **326** 699
- [49] Di Castro D, Bianconi G, Colapietro M, Pifferi A, Saini N L, Agrestini S and Bianconi A 2000 *Eur. Phys. J. B* **18** 617
- [50] Chakravarty S, Kee H J and Völker K 2004 *Nature* **428** 53–5
- [51] Peng Y Y *et al* 2017 *Nat. Phys.* **13** 1201